domly between 5208 and 5017 Å. Although the lines are not identified, the strength of the fluorescence and the beat structure observed ensured that these lines were excited from $v=0$, $J=40-90$ ground-state levels. The wave numbers of the transitions were measured to within 0.15 cm^{-1}. The analysis of $I_\sigma(t)-I_\pi(t)$ provided the g_J factors with an accuracy of about 8%. The seven values are plotted in Fig. 3 along with the g_J values of the $(J,v)=(27,62)$ and the $(J,v)=(79,40)$ levels. They are scaled to enable a comparison with the spin-rotation data G_{exp}. Figure 3 displays an excellent agreement between the energy dependence of G_{exp} and g_J, demonstrating the proportionality between these coupling constants. Using a least-squares fit to the hf coupling data G_{exp}, we find for the energy dependence of g_J in the energy range investigated $g_J=A/(E_c-E)$, with $A=-2.3(2)\times10^2\mu_N$ cm^{-1} and $E_c=4391(40)$ cm^{-1}.

The detection of Zeeman quantum beats has proven to be a valuable new spectroscopic tool for the direct measurement of Landé factors in molecular iodine. The only other method reported to measure g factors in the excited B state is the Hanle effect with modulated light.[2] Unlike quantum-beat spectroscopy, this technique is limited to levels with rather large g_J and long lifetime τ and therefore to investigations very close to the dissociation limit. Further investigations with these methods should provide a detailed survey of the magnetic interactions in the excited states of iodine and other molecules.

*Work supported by the National Science Foundation under Grant No. GP-28415.

†Present address: Department of Physics, Free University, Berlin, West Germany.

[1]M. Broyer and J. C. Lehmann, Phys. Lett. 40A, 43 (1972).

[2]J. C. Keller, M. Broyer, and J. C. Lehmann, C. R. Acad. Sci., Ser. B 277, 369 (1973).

[3]M. Sorem, thesis, Stanford University Microwave Laboratory Report No. 2082, 1972 (unpublished).

[4]S. Haroche, J. A. Paisner, and A. L. Schawlow, Phys. Rev. Lett. 30, 948 (1973).

[5]W. Gornik, D. Kaiser, W. Lange, J. Luther, and H. H. Schulz, Opt. Commun. 6, 327 (1972).

[6]M. D. Levenson and A. L. Schawlow, Phys. Rev. A 6, 10 (1972).

[7]G. Herzberg, *Spectra of Diatomic Molecules* (Van Nostrand Reinhold, New York, 1950).

[8]C. H. Townes and A. L. Schawlow, *Microwave Spectroscopy* (McGraw-Hill, New York, 1955).

[9]J. A. Paisner and R. Wallenstein, to be published.

[10]$G_{exp}=G^1-G^0$; G^0 and G^1 are the hyperfine coupling constants of the ground and excited levels. Except for low energies E, G^0 is very small compared to G^1 (Ref. 6).

Precision Measurement of the Rydberg Constant by Laser Saturation Spectroscopy of the Balmer α Line in Hydrogen and Deuterium*

T. W. Hänsch,† M. H. Nayfeh, S. A. Lee, S. M. Curry,‡ and I. S. Shahin§
Department of Physics, Stanford University, Stanford, California 94305
(Received 8 April 1974)

We have determined a new Rydberg value, $R_\infty=109\,737.314\,3(10)$ cm^{-1}, with an order of magnitude improvement in precision, by measuring the absolute wavelengths of resolved fine-structure components of the Balmer α line in hydrogen and deuterium, excited in a dc gas discharge. Doppler broadening was eliminated by saturation spectroscopy with a pulsed dye laser. An iodine-stabilized He-Ne laser was the wavelength standard. Possible sources of systematic errors have been carefully investigated.

We have determined the Rydberg constant with an almost tenfold improvement in accuracy over recent other experiments,[1,2] by measuring the absolute wavelength of the optically resolved $2P_{3/2}$-$3D_{5/2}$ component of the red Balmer line H_α of atomic hydrogen and D_α of deuterium in a Wood discharge. Doppler broadening was eliminated by saturation spectroscopy[3] with a pulsed, tunable, dye laser. An iodine-stabilized He-Ne laser served as the wavelength standard.[4] The same measurements provide a new precise value for the H_α-D_α isotope shift. We have also determined the splittings between the stronger fine-structure components in the optical spectrum to within a few megahertz.

The Rydberg constant, an important corner-

stone in the evaluation of the other fundamental constants, is related to the wavelengths in the spectra of one-electron atoms via Bohr's formula, corrected for finite nuclear mass, Dirac fine structure, and Lamb shifts.[5] Even the most recent wavelength measurements of hydrogen and deuterium discharge emission lines, using conventional high-resolution spectroscopy, were hampered by the particularly large Doppler broadening of these lines, even at cryogenic temperatures, and the resulting need for troublesome deconvolutions of blends of unresolved fine-structure components. The feasibility of a dramatically improved Rydberg measurement became apparent when we succeeded in resolving single fine-structure components of H_α in laser saturated absorption.[3]

The present measurement is based on these earlier qualitative experiments. A simplified optical scheme is given in Fig. 1. The saturation spectrometer (top) is essentially the same as before.[3] Hydrogen or deuterium is generated electrolytically and continuously pumped through a Wood-type dc discharge tube, where it is excited to the atomic $n=2$ state (1-m-long folded Pyrex tube, 8 mm diameter, 0.1–1 Torr, cold Al cathode, 8–20 mA, electronic switch for afterglow measurements). The saturated absorption is observed in a 15-cm-long center section of the positive column (typical absorption at resonance, 20–50%). The light source is a nitrogen-laser–pumped dye laser[6] with an external confocal-filter interferometer [71 pulses per second, 30-MHz linewidth (full width at half-maximum), 8-nsec pulse length]. It provides two, weak, probe beams (1 mm diameter, 4 mm apart, symmetric with respect to the tube axis, peak power < 5 mW) and a counterpropagating, alternately chopped, saturating beam, which overlaps one of the probes in the discharge (crossing angle, 2 mrad). At exact resonance the two counterpropagating waves are interacting with the same atoms, those with essentially zero axial velocity, and the saturating beam can bleach a path for its probe, producing a saturation signal. The use of the second reference probe in a differential-detection scheme reduces the noise due to randomly fluctuating laser amplitudes which exhibit an exponential pulse-height distribution after passsing the external interferometer.[7]

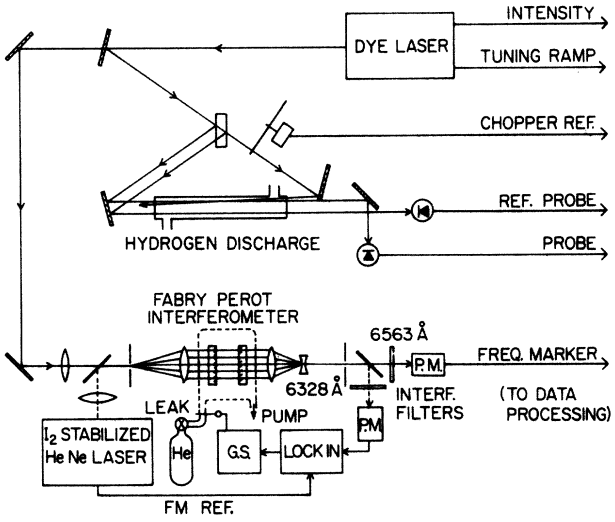

FIG. 1. Optical scheme of saturation spectrometer and wavelength comparator.

To measure absolute wavelengths, part of the dye-laser light is sent through a fixed Fabry-Perot interferometer (bottom), whose spacing is accurately known in terms of the He-Ne–laser standard wavelength. While the saturation spectrum is produced by slowly scanning the laser frequency across the line profile, the resulting transmission maxima are recorded simultaneously as wavelength markers.

The iodine-stabilized He-Ne laser is similar to that described by Schweitzer *et al.*[4] Its frequency is electronically locked to the n hyperfine component of the coincident $^{129}I_2$ absorption line. This wavelength has been measured in terms of the ^{86}Kr standard to within 1.4 parts in 10^9. The He-Ne–laser beam and part of the dye-laser beam are focused through a common pinhole (140 μm diameter) and sent through a collimating quartz lens ($f=105$ cm) perpendicularly into the plane Fabry-Perot interferometer. Feedback into the laser cavity is minimized by an optical isolator, an attenuator, and random phase modulation of the back-reflected light with a vibrating mirror. The transmitted light passes through a Galilean telescope (20×), and a second pinhole (1 mm diameter) in its image plane eliminates any ghost fringes. The two laser beams are finally split by filters and monitored by separate photomultipliers.

The interferometer is mounted in an air-tight chamber with high-quality windows for pressure tuning. The plates (coating: Ag, $T=5\%$, or Al, $T=11\%$) are flat to within $\lambda/200$ over the utilized area (1 cm diameter) and are separated by a spring-loaded Invar spacer of up to 64 mm length. Such a large spacing greatly facilitates an accurate wavelength comparison. Earlier interfero-

metric measurements of gas-discharge emission lines required much shorter spacers to avoid multiple interferometer orders within the line profile.

The spacer length l can be measured mechanically to within a few micrometers. For a more precise determination, to within 1 order number, we compared the measured relative positions of the Fabry-Perot fringes of up to eight known spectral lines (Cd and Hg) with numerical computations. During the experiment, the interferometer is kept in exact resonance (± 1 MHz) with the He-Ne laser by manually controlling the pressure of the tuning gas. A sensitive indicator is the zero crossing of the dispersion-shaped differentiated Fabry-Perot resonance observed with a lock-in detector, utilizing the frequency modulation of the He-Ne laser (2-MHz sweep).

The strong $2P_{3/2}$-$3D_{5/2}$ component (line 1 in Fig. 2) was chosen for the absolute wavelength measurement because it exhibits the smallest hyperfine splitting. The effect of tuning nonlinearities is minimized by selecting the order of the pressure-tuned interferometer so that a marker resonance appears in near coincidence with this line. The accuracy of earlier wavelength measurements is sufficient to identify uniquely the order number n of this marker, and the precise wavelength can be determined from the relative separation of the marker and the fine-structure line.

Six parameters, as indicated in Fig. 1, are stored for each laser pulse in digital form on a magnetic disk memory for later processing with a small laboratory computer. The saturation signal is computed, without model-dependent normalization, by taking the intensity difference $I_p - I_r$ of probe and reference probe in the presence of the saturating beam, and subtracting a correction due to imperfect balancing of the two probes. This correction, $\langle (I_p^0 - I_r^0)/I^0 \rangle I$, is calculated from the neighboring parameter values without saturating beam (labeled by superscript zero). The saturation spectrum is obtained by sorting these signals according to tuning ramp, i.e., laser frequency, into an 800-element array. A corresponding array is calculated for the normalized wavelength-marker signal. These spectra are smoothed, without introducing systematic line shifts, by convolution with a Gaussian or Lorentzian profile. The spectrum shown in Fig. 2 was obtained by averaging over six individual runs of 6 min duration.

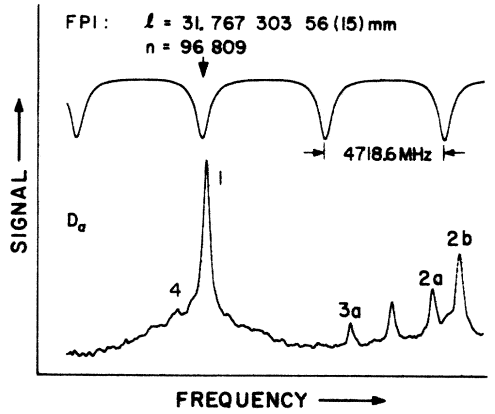

FIG. 2. Saturation spectrum of Balmer line D_α, with simultaneously recorded transmission maxima of Fabry-Perot interferometer.

Both the center of gravity and the center of area were calculated for that part of the fine-structure line which reaches above half-maximum. The line profile is sufficiently symmetric so that these two values are in good agreement, and the cutoff level ensures that any line shifts due to the weak neighboring $2P_{3/2}$-$3D_{3/2}$ component (line 4, Fig. 2) and its intermediate crossover line remain negligible. This simple procedure has the advantage of not depending on any line-profile models.

A series of wavelength measurements was performed for hydrogen and deuterium. The optical geometry was frequently optimized in between runs to randomize any alignment errors. The refractive-index dispersion of the tuning gas (N_2 or He) was taken into account in the data evaluation.[8] Most data were taken with a spacer of 63.8 mm length. It was confirmed, however, that a shorter 31.8-mm spacer gives the same results to within 1 standard deviation. A correction of 8 parts in 10^9 (for the longer spacer) was subtracted from the wavelengths obtained with the Ag etalon coatings to account for a wavelength-dependent phase change in reflection.[1]

Measurements in light hydrogen require an additional correction due to unresolved hyperfine splitting because saturation spectroscopy at low intensity weights the line components with the squares of their oscillator strengths. An upward wavelength shift of 3.6 parts in 10^9 is expected for the $2P_{3/2}$-$3D_{5/2}$ components, if crossover lines are absent. If we assume the presence of additional unresolved crossover lines with a magnitude equal to the geometric means of their parents, then we expect a shift of 4.2 parts in 10^9 for quadratic response (and of 2.1 parts in 10^9 for linear response). In the final analysis, we

applied a correction of 4.2 parts in 10^9 to the hydrogen data. The correction for deuterium is negligible.

Several other sources of possible systematic errors have been carefully studied. To investigate possible Stark shifts we measured the wavelength both with running discharge and in the afterglow, 0.5 μsec after electronically stalling the discharge. No systematic line shifts could be found within standard deviations of 2 parts in 10^8. A shift of -4.5 parts in 10^9 is expected for a dc field of 10 V/cm in the positive column of the discharge.[9] We have experimental evidence that the Stark effect due to the microfields of free electrons and ions in the afterglow is smaller than that. A field of 10 V/cm is sufficient for Stark mixing of the closely spaced hydrogen levels $3P_{3/2}$ and $3D_{3/2}$,[10] and a corresponding crossover signal has been observed halfway between the lines $2S_{1/2}$-$3P_{3/2}$ (line 2a, Fig. 2) and $2P_{1/2}$-$3D_{3/2}$ (line 2b, Fig. 2), if the discharge is running. This crossover signal is essentially absent in the afterglow measurements. A Stark-shift correction of 4.5 parts in 10^9 was applied to wavelengths measured with running discharge.

For possible pressure shifts we established an experimental upper limit of (13 parts in 10^9)/Torr, or 2 parts in 10^9 at the typical pressure of 0.15 Torr, by comparing wavelength measurements at hydrogen pressures of 0.15, 0.3, and 0.44 Torr. Intensity-dependent light shifts on the order of (0.5 parts in 10^{10})/(mW/mm^2) are theoretically expected because of the weak neighboring fine-structure lines $2P_{3/2}$-$3D_{3/2}$ (line 4, Fig. 2) and $2P_{3/2}$-$3S_{1/2}$.[11] Sorting of the saturation spectra according to laser pulse height into eight ranges from 2 to 180 mW/mm^2 peak power gave an experimental upper limit for such shifts of (2 parts in 10^{10})/(mW/mm^2).

The absence of unknown systematic errors was further confirmed by optical measurements of the intervals between different fine-structure components of H_α. Closely spaced frequency markers were generated with a confocal calibration interferometer of 200-MHz free spectral range. For the interval between lines $2P_{1/2}$-$3D_{3/2}$ and $2S_{1/2}$-$3P_{3/2}$ (lines 2b and 2a, Fig. 2), measured in the afterglow, we obtained 1052.7(1.7) MHz; and for the interval between $2P_{1/2}$-$3D_{3/2}$ and $2P_{3/2}$-$3D_{5/2}$ (lines 2b and 1), 9884.5(2.9) MHz. Both values agree within their error limits with theoretical values, and seem to give an experimental confirmation for the expected small $3D_{3/2}$-$3P_{3/2}$ Lamb shift (5.3 MHz).[10]

In the final data analysis we averaged the wavelengths measured under various experimental conditions, so that the standard deviation gives some measure for residual systematic errors. For the $2P_{3/2}$-$3D_{5/2}$ component of H_α we determine an inverse vacuum wavelength of 15 233.070 21(9) cm^{-1} from 17 individual spectra, where the uncertainty is 1 standard deviation. For the corresponding D_α line we obtain 15 237.215 38(8) cm^{-1} from 33 spectra. The resulting H_α-D_α isotope shift is 4.145 17(12) cm^{-1}.

To determine the Rydberg constant, we fitted the measured wave numbers with calculated wavenumbers, which are proportional to an assumed Rydberg value. We used calculations by Erickson,[12] which are similar to those by Garcia and Mack,[13] but take the 1973 adjustments of the fundamental constants into account. In this way we obtain $R_\infty = 109\,737.313\,0(6)$ cm^{-1} for H_α and $R_\infty = 109\,737.315\,0(6)$ cm^{-1} for D_α. If we ignore the small discrepancy between the two isotopes and combine all individual measurements, we arrive at $R_\infty = 109\,737.314\,3(4)$ cm^{-1}, with a standard deviation of 4 parts in 10^9. The final, larger rms error of 0.001 cm^{-1} or 1 part in 10^8 includes the uncertainties of the systematic corrections and residual systematic errors. The conservatively estimated contributions are as follows (parts in 10^9): phase dispersion of etalon coatings, 4; refractive index of tuning gas, 2; wavelength standard, 4; unresolved hyperfine splitting, 4; Stark shifts, 3; intensity shifts, 2; and pressure shifts, 2. The new Rydberg value is only slightly outside the error limits of Kibble *et al.*'s recent measurement[1] and agrees with Kessler's result.[2]

For future refinements of the present experiment it may be desirable to replace the discharge by a beam of metastable hydrogen atoms. A very accurate Rydberg value can also be expected, when the new technique of two-photon spectroscopy without Doppler broadening[14] is applied to the $1S$-$2S$ transition in hydrogen.

We are indebted to Professor A. L. Schawlow, Professor G. W. Series, and to Dr. B. Kibble for many stimulating discussions and valuable advice, and we are grateful to Professor G. Erickson for making his computer calculations available to us prior to publication.

*Portions of this work supported by the National Science Foundation under Grant No. GP-28415, by the U. S. Office of Naval Research under Contract No. ONR-

0071, and by a Precision Measurement Grant from the National Bureau of Standards.

†Alfred P. Sloan Fellow, 1973–1975.

‡Present address: Department of Physics, University of Texas at Dallas, Dallas, Tex. 75230.

§Present address: Department of Physics, University of Jordan, Amman, Jordan.

[1]B. P. Kibble, W. R. C. Rowley, R. E. Shawyer, and G. W. Series, J. Phys. B: Proc. Phys. Soc., London 6, 1079 (1973).

[2]E. G. Kessler, Phys. Rev. A 7, 408 (1973).

[3]T. W. Hänsch, I. S. Shahin, and A. L. Schawlow, Nature (London), Phys. Sci. 235, 63 (1972).

[4]W. G. Schweitzer, Jr., E. G. Kessler, Jr., R. D. Deslattes, H. P. Layer, and J. R. Whetstone, Appl. Opt. 12, 2827 (1973).

[5]G. W. Series, Contemp. Phys. 14, 49 (1974).

[6]T. W. Hänsch, Appl. Opt. 11, 895 (1972).

[7]S. M. Curry, R. Cubeddu, and T. W. Hänsch, Appl. Phys. 1, 153 (1973).

[8]*Landolt-Börnstein: Zahlenwerte and Funktionen*, edited by K.-H. Hellwege and A. M. Hellwege (Springer, Berlin, 1962), Vol. II, Pt. 8, p. 6-897.

[9]J. A. Blackman and G. W. Series, J. Phys. B: Proc. Phys. Soc., London 6, 1090 (1973).

[10]H. A. Bethe and E. E. Salpeter, in *Encylopedia of Physics*, edited by S. Flügge (Springer, Berlin, 1957), Vol. XXXV.

[11]M. Mizushima, Phys. Rev. 133, A414 (1964).

[12]G. Erickson, to be published.

[13]J. D. Garcia and J. E. Mack, J. Opt. Soc. Amer. 55, 654 (1965).

[14]T. W. Hänsch, K. C. Harvey, G. Meisel, and A. L. Schawlow, to be published.

Cascade Anticrossing Measurement of the Anomalous Hyperfine Structure of the 4^2D State of Rubidium*

K. H. Liao, L. K. Lam, R. Gupta, and W. Happer

Columbia Radiation Laboratory, Department of Physics, Columbia University, New York, New York 10027

(Received 29 April 1974)

A new technique, cascade anticrossing spectroscopy, has been developed to determine the effective values of $\langle r^{-3}\rangle$ for the spin-dipole, orbital, contact, and quadrupole hyperfine interaction terms for the 4^2D state of Rb. They are, in units of 10^{24} cm^{-3}, $\langle r^{-3}\rangle_d = -0.36(8)$, $\langle r^{-3}\rangle_l = +0.20(2)$, $\langle r^{-3}\rangle_c = -4.3(1)$, and $\langle r^{-3}\rangle_q = +0.79(66)$, respectively. The negative value of $\langle r^{-3}\rangle_d$ and the unexpectedly large value of $\langle r^{-3}\rangle_c$ are surprising. The fine-structure splitting has been measured to be $-13\,360.9(8)$ MHz.

Recently, experimental investigations of the D-state hyperfine structures of alkali atoms[1] have revealed that many $D_{5/2}$ states have anomalous negative magnetic-dipole coupling constants. In order to gain a better understanding of these anomalies we have used a new spectroscopic technique, cascade anticrossing spectroscopy, to determine the complete hyperfine Hamiltonian for the 4^2D state of rubidium. The results of this work are quite surprising. The core polarization of the $4D$ state is substantially larger than the core polarization of any of the P states of rubidium, and the effective value of $\langle r^{-3}\rangle$ for the dipole contribution to the hyperfine structure is *negative*. Although many instances are known[2] where the effective values of $\langle r^{-3}\rangle$ for the dipole and orbital contributions to the hyperfine structure are not the same, the differences seldom exceed 10%, and we are not aware of any other report of a negative value for $\langle r^{-3}\rangle$.

The magnetic dipole and electric quadrupole contribution to the hyperfine-structure Hamiltonian of a hydrogenic atom can be written as

$$\mathcal{H}_{\rm hfs} = \mathcal{H}_l + \mathcal{H}_d + \mathcal{H}_c + \mathcal{H}_q . \tag{1}$$

The electric quadrupole contribution is

$$\mathcal{H}_q = \frac{2LQe^2}{2L+3}\langle r^{-3}\rangle_q \frac{3(\vec{\mathbf{L}}\cdot\vec{\mathbf{I}})^2 + \frac{3}{2}(\vec{\mathbf{L}}\cdot\vec{\mathbf{I}}) - L(L+1)I(I+1)}{2L(2L-1)I(2I-1)}, \tag{2}$$

where Q is the nuclear quadrupole moment. The orbital contribution is

$$\mathcal{H} = [(2\mu_B\mu_I)/I]\langle r^{-3}\rangle_l \vec{\mathbf{L}}\cdot\vec{\mathbf{I}} \tag{3}$$

and the dipole contribution is

$$\mathcal{H}_d = \frac{4\mu_B\mu_I}{I}\langle r^{-3}\rangle_d \frac{L(L+1)}{(2L-1)(2L+3)}\left[\vec{\mathbf{S}}\cdot\vec{\mathbf{I}} - 3\left\{\frac{\vec{\mathbf{S}}\cdot\vec{\mathbf{L}}\vec{\mathbf{L}}\cdot\vec{\mathbf{I}} + \vec{\mathbf{I}}\cdot\vec{\mathbf{L}}\vec{\mathbf{L}}\cdot\vec{\mathbf{S}}}{2L(L+1)}\right\}\right]. \tag{4}$$